Heliyon 10 (2024) e35476

Contents lists available at ScienceDirect

Heliyon

journal homepage: www.cell.com/heliyon

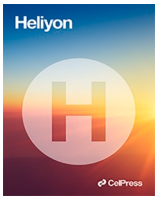

Research article

Growth differentiation factor-15 as a biomarker of coronary microvascular dysfunction in ST-segment elevation myocardial infarction

Rui Tian [a,b,c,d,e], Zerui Wang [a,b,c,d,e], Shenglin Zhang [a,b,c,d,e], Xiaojun Wang [a,b,c,d,e], Yiwen Zhang [a,b,c,d,e], Jiaquan Yuan [a,b,c,d,e], Jiajun Zhang [a,b,c,d,e], Feng Xu [a,b,c,d,e], Yuguo Chen [a,b,c,d,e], Chuanbao Li [a,b,c,d,e,*]

[a] *Department of Emergency Medicine, Qilu Hospital of Shandong University, Jinan ,250012, China*
[b] *Shandong Provincial Clinical Research Center for Emergency and Critical Care Medicine, Institute of Emergency and Critical Care Medicine of Shandong University, Chest Pain Center, Qilu Hospital of Shandong University, Jinan ,250012, China*
[c] *Key Laboratory of Emergency and Critical Care Medicine of Shandong Province, Key Laboratory of Cardiopulmonary-Cerebral Resuscitation Research of Shandong Province, Shandong Provincial Engineering Laboratory for Emergency and Critical Care Medicine, Qilu Hospital of Shandong University, Jinan ,250012, China*
[d] *Shandong Key Laboratory: Magnetic Field-free Medicine & Functional Imaging, Qilu Hospital of Shandong University, Jinan ,250012, China*
[e] *NMPA Key Laboratory for Clinical Research and Evaluation of Innovative Drug, Qilu Hospital of Shandong University, Jinan ,250012, China*

ARTICLE INFO

Keywords:
Growth differentiation factor-15
ST-Segment elevation myocardial infarction
Percutaneous coronary intervention
Coronary microvascular dysfunction
No-reflow phenomenon
Hemodynamics

ABSTRACT

Background: The predictive value of growth differentiation factor-15 (GDF-15) in coronary microvascular dysfunction (CMD) following primary percutaneous coronary intervention (PPCI) in ST-segment elevation myocardial infarction (STEMI) patients is unclear.

Methods: This study continuously recruited STEMI patients treated with PPCI at the Chest Pain Center of Qilu Hospital of Shandong University from April 2023 to December 2023. Blood samples were taken before PPCI and the level of circulating GDF-15 was measured by enzyme-linked immunosorbent assay (ELISA), and the patients were divided into CMD and Control group according to angiographic microvascular resistance (AMR) (cut-off value 2.50 mmHg*s/cm). The differences in GDF-15 expression levels between the two groups were compared, and the predictive value of GDF-15 for CMD was systematically evaluated.

Results: A total of 134 patients, with an average age of 59.78 ± 12.69 years and 75.37 % being male, were included in this study. Multivariable logistic regression revealed a significant association between GDF-15 and CMD (adjusted OR = 2.505, 95 % CI: 1.661–3.779, $P < 0.001$). The area under the curve (AUC) of GDF-15 for CMD was 0.782 (95 % CI: 0.704–0.861), with a sensitivity of 0.795 and specificity of 0.643 in predicting CMD in PPCI. The AUC of the GDF-15 model (Model With GDF-15) was 0.867 (95 % CI: 0.806−0.928), significantly outperforming the clinical baseline model (Model Without GDF-15) (Δ AUC = 0.079, 95 % CI: 0.020–0.138, $P = 0.009$). Furthermore, the net reclassification improvement (NRI) was 0.854 (95 % CI: 0.543–1.166, $P < 0.001$), and the integrated discrimination improvement (IDI) was 0.151 (95 % CI: 0.089–0.213, $P < 0.001$).

* Corresponding author. Qilu Hospital of Shandong University, 107 Wenhua Xi Road, Jinan, Shandong ,250012, China.
E-mail address: bao2460@126.com (C. Li).

https://doi.org/10.1016/j.heliyon.2024.e35476
Received 30 April 2024; Received in revised form 4 July 2024; Accepted 29 July 2024
Available online 30 July 2024

Conclusions: GDF-15 can serve as a biomarker for predicting the development of CMD in STEMI patients undergoing PPCI.

1. Introduction

Acute ST-segment elevation myocardial infarction (STEMI) represents a critical type of acute coronary syndrome (ACS) and a leading cause of death and disability globally [1]. Primary percutaneous coronary intervention (PPCI) is superior to thrombolytic therapy in quickly and effectively opening the infarct-related artery (IRA), thereby preserving left ventricular ejection function and enhancing patient survival rates [2]. Consequently, PPCI has emerged as the favored method for reinstating coronary blood flow in STEMI patients [3]. Nevertheless, post-IRA opening, 5 %–50 % of patients may develop coronary microvascular dysfunction (CMD) [4], including the no-reflow phenomenon (NRP), which escalates the likelihood of major adverse cardiovascular events (MACE) and augments in-hospital mortality, significantly compromising STEMI patient outcomes [5].

At present, prevalent CMD diagnostic approaches during PPCI encompass the thrombolysis in myocardial infarction flow grade (TFG) and the corrected TIMI frame count (cTFC), yet neither offers a precise, objective quantitative assessment [6]. Techniques like intracoronary Doppler or thermodilution enable measurement of the index of microcirculatory resistance (IMR) and coronary flow reserve (CFR), which accurately mirror the state of coronary microcirculation. However, their intricate nature and substantial costs have hampered widespread clinical adoption [7]. Lately, the angiographic microvascular resistance (AMR), derived from quantitative flow ratio (QFR) technology, has emerged as a superior quantitative measure for assessing myocardial ischemia, outperforming both TIMI and cTFC. AMR circumvents the drawbacks of IMR and CFR and has demonstrated significant accuracy and prognostic utility in evaluating CMD in STEMI patients [8–11].

Growth differentiation factor-15 (GDF-15), belonging to the transforming growth factor-β (TGF-β) superfamily, is pivotal in vascular development and remodeling, guiding processes like cell proliferation and differentiation [12]. GDF-15 is naturally abundant in specific tissues like the prostate and placenta, with minimal cardiovascular expression under normal conditions. However, during pathological events such as ischemia-reperfusion injury and hypertension, or amidst environmental stress, GDF-15 expression markedly increases in vascular tissues, influencing vascular cell proliferation, apoptosis, inflammation, remodeling, and angiogenesis [13]. Extensive studies reveal that GDF-15 levels are elevated in acute myocardial infarction (AMI) patients, serving as an independent prognostic marker for 30-day mortality post-percutaneous coronary intervention (PCI) in STEMI cases [14,15]. Its utility in STEMI risk

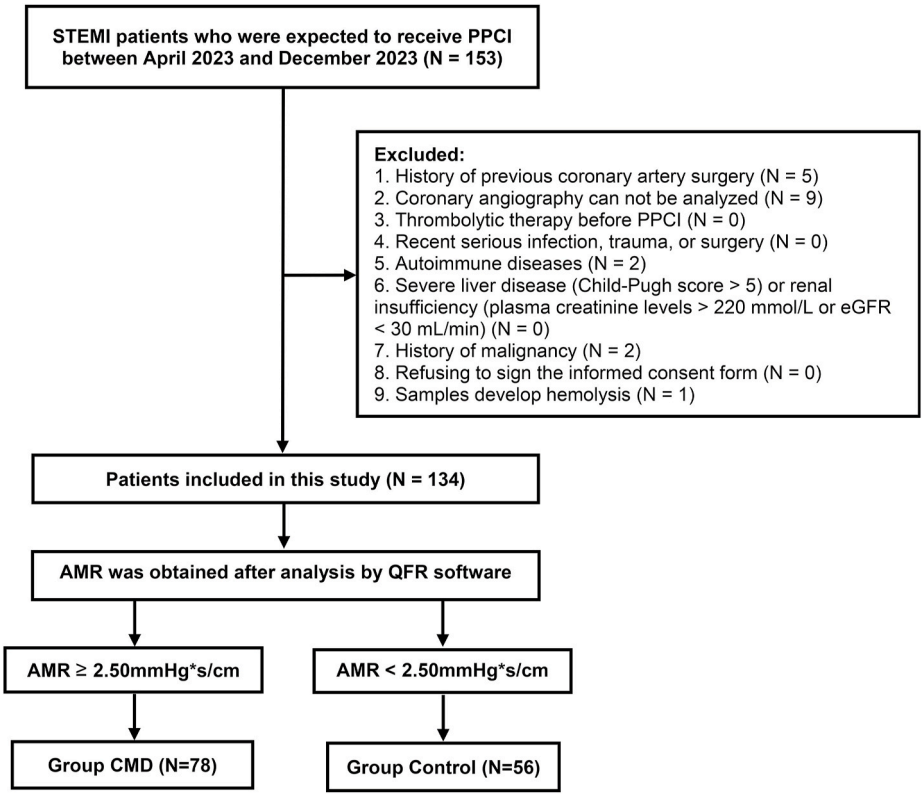

Fig. 1. Process of selection and grouping.

stratification underscores its potential as a novel biomarker, holding significant clinical relevance for both immediate and extended patient prognoses.

2. Materials and methods

Ethics approval

This study was approved by the Scientific Research Ethics Committee of Qilu Hospital of Shandong University (KYLL-202212-013-1) and conducted in accordance with the guidelines of the 1964 Helsinki Declaration [16], and all participating patients provided relevant written informed consent.

2.1. Study participants

This study was a single-center, prospective, observational study that continuously enrolled STEMI patients who were expected to receive PPCI treatment from April 2023 to December 2023 in the Chest Pain Center of Qilu Hospital of Shandong University. Inclusion criteria: (1) 18 years $\leq$ age; (2) The diagnostic criteria for STEMI are based on the Fourth Universal Definition of Myocardial Infarction [17]; (3) Onset to PPCI $\leq$12 h; (4) The subject voluntarily participates in the study and has signed the informed consent form. Exclusion criteria: (1) History of previous coronary artery surgery; (2) Coronary angiography can not be analyzed; (3) Thrombolytic therapy before PPCI; (4) Recent serious infection, trauma, or surgery; (5) Autoimmune diseases; (6) Severe liver disease (Child-Pugh score >5) or renal insufficiency (plasma creatinine levels >220 mmol/L or eGFR <30 mL/min); (7) History of malignancy; (8) Refusing to sign the informed consent form; (9) Samples develop hemolysis. In this study. Ultimately, 153 patients with acute STEMI were screened, of which 9 patients had coronary angiography data that could not be further analyzed, 5 patients with a history of previous PPCI or coronary artery bypass grafting (CABG), 2 patients with a history of malignancy, 2 patients with rheumatic immune diseases, and 1 patient with hemolysis in blood samples, and the final number of patients included in the study was 134 (Fig. 1).

2.2. Analysis of coronary angiography and grouping criteria

In this study, patients were categorized into two groups: CMD group and Control group, based on the occurrence of CMD in STEMI patients after PPCI treatment. The diagnostic criteria for CMD were determined by AMR $\geq$2.50 mmHg*s/cm, calculated using QFR technology [10,18]. All coronary angiography was reviewed by two experienced interventional cardiologists and two experienced QFR testers using the QFR detector (AngioPlus Core, version V3, Shanghai Pulse Medical Technology Co., Ltd., Shanghai, China). The researchers involved in the analysis were blinded to the treatment options received by the patients. The single-view μQFR was calculated first by selecting the best angiography with minimal vascular overlap. The QFR software automatically outlined the contour of the coronary artery lumen, calculated the contrast flow rate by dividing the length of the vascular centerline by the contrast filling time, and then converted it to hyperemic flow velocity (Velocityhyp). Frames with good contrast filling and fully exposed lumen profiles were chosen for analysis. The software automatically delineated the lumen boundaries of the interrogated vessels and major lateral branches, and reconstructed the reference vessel diameters following Murray's bifurcation fractal law [19]. Based on the hydrodynamic equations, the pressure drop was calculated using the given Velocityhyp as the boundary condition to determine the distal coronary pressure (Pd). The μQFR was then calculated as the ratio of Pd to the mean aortic pressure (Pa), assuming Pa to be 86 mmHg during maximum congestion. Additionally, the AMR was calculated as the ratio of Pd to Velocityhyp, resulting in AMR = Pd/Velocityhyp = Pa × μQFR/Velocityhyp [10,20] (Fig. S1).

2.3. Treatment regimen

All patients were given oxygen, sedation, bed rest, continuous electrocardiogram (ECG) and blood pressure monitoring, and oxygen saturation monitoring immediately after admission. According to current guidelines for the treatment of STEMI [21], all patients should be given a loading dose of aspirin 300 mg and clopidogrel 300 mg as a dual antiplatelet agent immediately after diagnosis, and given an intravenous bolus of 70–100 units/kg of unfractionated heparin. Coronary angiography, drug coated balloon (DCB) or drug eluting stent (DES) were performed on all STMEI patients through the radial artery pathway using a 6F contrast catheter with Omnipaque350 (350 mg/100 ml) and a GEINNOVA 3100 digital subtraction imaging machine and its image analysis system, with an image acquisition speed of 15 frames per second and a playback speed of 15 frames per second. Coronary interventionists decide on the use of drugs such as thrombus aspiration, balloon dilation, stent implantation, and GP IIb/IIIa receptor antagonists.

2.4. Clinical data collection

(1) General information collection: age, gender, body mass index (BMI), heart rate (HR), systolic blood pressure (SBP), diastolic blood pressure (DBP), Killip grade, smoking history, alcohol history, hypertension history, diabetes mellitus history and coronary artery disease (CAD) family history were obtained through admission records. (2) Laboratory indicators collection: myocardial markers [N-Terminal pro-B-type natriuretic peptide (NT-proBNP), creatine kinase isoenzyme (CK-MB), high-sensitivity troponin I (hs-TnI)], blood lipid profile [cholesterol (Cho), high density lipoprotein-cholesterol (HDL-C), low density lipoprotein-cholesterol (LDL-C), triglycerides (TG)], white blood cell count (WBC), fibrinogen (FIB), and D-Dimer (DD-i) were collected by the laboratory department of

our hospital. (3) Surgical data collection: infarction-related arteries (IRA), surgery time, thrombus aspiration, pre-dilation, post-dilation, number of stents, mean stent length, mean stent diameter, and intraoperative medications (nicorandil and tirofiban) were obtained from surgical records.

2.5. Laboratory analysis

After arterial puncture in the catheter intervention operating room and before PPCI treatment, 3 mL of arterial blood from all study subjects was collected into an EDTA anticoagulant tube and immediately transported to the laboratory, centrifuged at 1000g, 4 °C for 15 min, and the supernatant was transferred to a cryovial tube and stored at −80 °C. According to the instructions of the human GDF-15 ELISA (enzyme-linked immunosorbent assay, ELISA) kit (Wuhan Yunclone Technology Co., Ltd., Cat. No. SEC034Hu), the plasma level of GDF-15 was detected by ELSIA, each sample was taken in triplicate, and the optical density (optical density, OD). The coefficient of variation within the assay is <10 % and the coefficient of variation between assays is <12 %.

2.6. Follow-up

All patients were followed up for 30 days after PPCI, and face-to-face communication was used to obtain the occurrence of MACE during hospitalization, and outpatient review records and telephone communication were used to obtain the occurrence of MACE after discharge. Follow-up endpoints were MACE, including cardiac death, recurrent angina or myocardial infarction (MI), heart failure (HF), malignant arrhythmias, and non-fatal stroke. (1) Cardiac death: death caused by severe cardiac dysfunction or failure due to various heart diseases or injuries. (2) Angina: a clinical syndrome in which transient myocardial ischemia triggered by various reasons such as fatigue or emotion leads to discomfort or pressure in the precordial area. (3) MI: the same as the diagnostic criteria for AMI in the Fourth Edition of the Global Definition of Myocardial Infarction. (4) HF: a syndrome characterized by pulmonary and systemic congestion due to various cardiac structural or functional diseases leading to impaired ventricular filling or ejection function, mainly manifested as dyspnea and limited physical activity, and confirmed by elevated natriuretic peptide levels or objective evidence of pulmonary or systemic congestion, including new-onset HF and worsening of HF. (5) Malignant arrhythmia: including frequent premature ventricular complex, ventricular tachycardia, ventricular flutter, ventricular fibrillation and third-degree atrioventricular block. (6) Stroke: including ischemic and hemorrhagic stroke.

2.7. Statistical analyses

Statistical analysis was performed by using R (version 4.1.3; The R Project for Statistical Computing). The Shapiro-Wilk test was used to test the normality of the data, and the normalized distribution of continuous data was represented by $\bar{x} \pm s$, and the *t*-test of two independent samples was used for comparison between groups. The non-normally distributed continuous data were represented by the median and interquartile ranges [M (P25,P75)], and the two-independent-sample nonparametric test (Mann-Whitney U rank-sum test) was used for comparison between groups. Count data were expressed as cases and rates [n (%)], and comparisons between groups were performed using either the chi-square test or Fisher's exact test. Univariate and multivariable logistic regression were used to analyze the associated variables of CMD after PPCI in STEMI patients. The GDF-15 was divided into four equal parts according to the level, and two different models, univariate and multivariable logistic, were used to further evaluate the correlation between GDF-15 and CMD. Correlation analysis between continuous variables was calculated using the Spearman test and based on sex, age, BMI, Killip grade, IRA, and LDL-C were analyzed to further validate the association of GDF-15 for CMD in different patients. The receiver operating characteristic curve (ROC) and area under the curve (AUC) were used to evaluate the predictive value of GDF-15 for CMD. Based on the clinical baseline data modeling, GDF-15 re-modeling was added on this basis, and the prediction performance of the two models was compared by calculating the Δ AUC, net reclssification improvement (NRI) and integrated discrimination improvement (IDI) to evaluate the incremental predictive value of GDF-15. In addition, the ROC of CMD was independently predicted according to GDF-15 and the optimal cut-off value was obtained by Youden index analysis, and the patients were divided into high-level group and low-level group for further analysis, and the cumulative probability curve of 30-day MACE was plotted by Kaplan-Meier method. All statistical tests were performed bilaterally, and $P < 0.05$ was used as the test level.

3. Results

3.1. Clinical and procedural characteristics

According to the inclusion and exclusion criteria formulated in this study, a total of 134 patients were finally included, and the patients with AMR value ≥ 2.50 mmHg*s/cm were classified as CMD group according to intraoperative coronary angiography analysis, and the rest were Control group. The incidence of CMD in this study was 58.2 %. A total of 78 patients were in the CMD group, with an average age of 61.19 ± 13.07 years, including 53 males and 25 females. A total of 56 patients were in the Control group, with an average age of 57.80 ± 11.98 years, including 48 males and 8 females. Compared with the Control group, the proportion of males (67.95 % vs. 85.71 %, $P = 0.031$), SBP (121.87 ± 19.93 mmHg vs. 132.43 ± 21.37 mmHg, $P = 0.004$) and DBP (75.55 ± 13.14 mmHg vs. 81.02 ± 12.2 mmHg, $P = 0.015$) in the CMD group were significantly smaller than those in the Control group, but the level of circulating GDF-15 (3.43 ± 1.03 ng/ml vs. 2.22 ± 1.13 ng/ml, $P < 0.001$), the proportion of Killip >1 (19.23 % vs. 5.36 %, $P = 0.039$) and the LCX ratio (16.67 % vs. 3.57 %, $P = 0.045$) were significantly higher than those in the Control group. There were no statistically

significant differences between the two groups in other variables (Table 1).

3.2. Association between the GDF-15 and CMD

(1) GDF-15 as a continuous variable: univariate logistic regression of CMD after PPCI treatment in STEMI patients showed that gender (OR = 0.353, 95 % CI: 0.146–0.858, $P = 0.021$), SBP (OR = 0.975, 95 % CI: 0.957–0.993, P = 0.005), DBP (OR = 0.967, 95 % CI: 0.940–0.994, $P = 0.019$), Killip (OR = 4.206, 95 % CI: 1.155–15.316, $P = 0.029$) and GDF-15 (OR = 2.686, 95 % CI: 1.836–3.929, $P < 0.001$) were influencing factors for CMD in STEMI patients treated with PPCI (Table 2). According to the results of univariate logistic regression, the covariates of $P < 0.10$ were included in the multivariable logistic regression, and the results showed that GDF-15 (adjusted OR = 2.505, 95 % CI: 1.661–3.779, $P < 0.001$) and IRA (adjusted OR = 0.305, 95 % CI: 0.113–0.829, $P = 0.020$) were independent influencing factors for the occurrence of CMD (Table 2). (2) GDF-15 as a categorical variable: patients were divided into four equal parts according to GDF-15 levels, and the Q1 group was used as a reference for the evaluation of the other groups. In Model U, univariate logistic regression showed that the OR of Q2 (OR: 4.886, 95 % Cl: 1.672–14.274, $P < 0.05$), Q3 (OR: 8.871, 95 % Cl: 2.910–27.042, $P < 0.001$) and Q4 (OR: 27.964, 95 % Cl: 7.354–106.332, $P < 0.001$) was significantly increased compared with Q1, and the trend was $P < 0.001$. In Model M, multivariable logistic regression showed that the adjusted OR of Q2 (adjusted OR: 5.830, 95 % Cl: 1.764–19.266, $P < 0.05$), Q3 (adjusted OR: 7.591, 95 % Cl: 2.231–25.825, $P < 0.05$) and Q4 (adjusted OR: 24.639, 95 % Cl:

Table 1
Baseline characteristics of the CMD and Control group.

Variables	Total (n = 134)	CMD (n = 78)	Control (n = 56)	*P*
Age (years)	59.78 ± 12.69	61.19 ± 13.07	57.80 ± 11.98	0.123
Male	101 (75.37)	53 (67.95)	48 (85.71)	0.031
BMI (kg/m2)	25.78 ± 3.92	25.34 ± 4.00	26.38 ± 3.77	0.129
HR (bpm)	76.35 ± 12.91	75.95 ± 12.25	76.91 ± 13.87	0.679
SBP (mmHg)	126.28 ± 21.12	121.87 ± 19.93	132.43 ± 21.37	0.004
DBP (mmHg)	77.84 ± 13.00	75.55 ± 13.14	81.02 ± 12.20	0.015
Killip				0.039
1	116 (86.57)	63 (80.77)	53 (94.64)	
>1	18 (13.43)	15 (19.23)	3 (5.36)	
Smoking	73 (54.48)	40 (51.28)	33 (58.93)	0.483
Drinking	54 (40.30)	29 (37.18)	25 (44.64)	0.490
Hypertension	77 (57.46)	45 (57.69)	32 (57.14)	0.999
Diabetes mellitus	37 (27.61)	25 (32.05)	12 (21.43)	0.246
CAD family history	16 (11.94)	10 (12.82)	6 (10.71)	0.920
GDF-15 (ng/ml)	2.92 ± 1.23	3.43 ± 1.03	2.22 ± 1.13	<0.001
Nt-proBNP (mmol/l)	760.15 (414.62, 1666.75)	730.15 (400.88, 1713.00)	777.20 (424.00, 1597.00)	0.933
CK-MB (ng/ml)	97.10 (22.17, 183.93)	105.95 (36.38, 174.15)	77.05 (14.78, 210.55)	0.359
hs-TnI (ng/l)	24212.83 (6828.22, 42163.72)	24212.83 (10103.95, 42270.08)	23330.00 (4283.84, 37806.44)	0.506
Cho (mmol/l)	4.45 (3.75, 5.22)	4.54 (3.78, 4.98)	4.32 (3.74, 5.48)	0.735
HDL-C (mmol/l)	1.07 (0.93, 1.28)	1.08 (0.95, 1.28)	1.07 (0.90, 1.23)	0.381
LDL-C (mmol/l)	2.74 (2.24, 3.40)	2.70 (2.26, 3.33)	2.81 (2.23, 3.56)	0.442
TG (mmol/l)	1.27 (1.01, 1.85)	1.26 (1.01, 1.75)	1.31 (1.02, 1.98)	0.491
WBC (109/l)	8.55 (6.51, 10.25)	8.96 (6.58, 10.44)	8.20 (6.38, 9.79)	0.230
FIB (μg/ml)	3.16 (2.76, 3.80)	3.13 (2.74, 3.69)	3.22 (2.79, 3.98)	0.309
DD-i (μg/ml)	0.30 (0.19, 0.51)	0.29 (0.19, 0.56)	0.32 (0.19, 0.43)	0.912
IRA				0.045
LAD	64 (47.76)	37 (47.44)	27 (48.21)	
LCX	15 (11.19)	13 (16.67)	2 (3.57)	
RCA	55 (41.04)	28 (35.90)	27 (48.21)	
Surgery time (mins)	45.00 (40.00, 55.00)	50.00 (40.00, 55.00)	45.00 (35.00, 51.25)	0.531
Thrombus aspiration	12 (8.96)	6 (7.69)	6 (10.71)	0.766
Pre-dilation	133 (99.25)	77 (98.72)	56 (100.00)	0.999
Post-dilation	95 (70.9)	55 (70.51)	40 (71.43)	0.999
Stent number				0.807
0	7 (5.22)	5 (6.41)	2 (3.57)	
1	102 (76.12)	58 (74.36)	44 (78.57)	
2	25 (18.66)	15 (19.23)	10 (17.86)	
Stent diameter (mm)	3.00 (2.50, 3.25)	2.94 (2.50, 3.25)	3.00 (2.50, 3.12)	0.650
Stent length (mm)	24 (19.62, 29.75)	24 (19.25, 29.00)	24 (19.88, 30.00)	0.560
Nicorandil	7 (5.22)	4 (5.13)	3 (5.36)	0.999
Tirofiban	15 (11.19)	11 (14.1)	4 (7.14)	0.326

Data are n (%), mean ± standard deviation, median (interquartile range).
CMD, coronary microvascular dysfunction; BMI, body mass index; HR, heart rate; SBP, systolic blood pressure; DBP. diastolic blood pressure; CAD, coronary artery disease; GDF-15, growth differentiation factor-15; NT-proBNP, N-terminal pro-brain natriuretic peptide; CK-MB, creatine kinase isoenzyme MB; hs-TnI, high-sensitivity Troponin-I; Cho, cholesterol; HDL-C, high-density lipoprotein cholesterol; LDL-C, low-density lipoprotein cholesterol; TG, triglycerides; WBC, white blood cell; FIB, fibrinogen; DD-i, D-dimer; IRA, infarct related artery; LAD, left anterior descending; LCX, left circumflex artery; RCA, right coronary artery.

Table 2
Logistic regression analysis.

	Univariate analysis						Multivariable analysis					
Variables	*β*	Wald	SE	OR	95%CI	*P*	*β*	Wald	SE	adjusted OR	95%CI	*P*
Age (years)	0.021	2.306	0.014	1.022	0.994–1.050	0.129						
Male	−1.040	5.287	0.452	0.353	0.146–0.858	0.021	−0.543	0.894	0.574	0.581	0.189–1.790	0.344
BMI (kg/m2)	−0.069	2.241	0.046	0.933	0.852–1.022	0.134						
HR (bpm)	−0.006	0.182	0.014	0.994	0.968–1.021	0.670						
SBP (mmHg)	−0.025	7.716	0.009	0.975	0.957–0.993	0.005	−0.023	2.260	0.016	0.977	0.948–1.007	0.133
DBP (mmHg)	−0.034	5.543	0.014	0.967	0.940–0.994	0.019	−0.017	0.397	0.027	0.983	0.933–1.036	0.529
Killip												
1												
>1	1.437	4.747	0.659	4.206	1.155–15.316	0.029	1.369	3.283	0.756	3.932	0.894–17.296	0.070
Smoking	−0.310	0.767	0.354	0.734	0.367–1.467	0.381						
Drinking	−0.309	0.753	0.357	0.734	0.365–1.476	0.386						
Hypertension	0.022	0.004	0.354	1.023	0.511–2.048	0.949						
Diabetes mellitus	0.548	1.820	0.406	1.730	0.780–3.834	0.177						
CAD family history	0.203	0.137	0.549	1.225	0.418–3.594	0.711						
GDF-15 (ng/ml)	0.988	25.925	0.194	2.686	1.836–3.929	<0.001	0.918	19.162	0.210	2.505	1.661–3.779	<0.001
Nt-proBNP (mmol/l)	0.000	0.574	0.000	1.000	1.000–1.000	0.449						
CK-MB (ng/ml)	0.000	0.011	0.002	1.000	0.997–1.003	0.915						
hs-TnI (ng/l)	0.000	0.000	0.000	1.000	1.000–1.000	0.988						
Cho (mmol/l)	−0.157	1.112	0.149	0.855	0.638–1.144	0.292						
HDL-C (mmol/l)	0.280	0.191	0.642	1.324	0.376–4.662	0.662						
LDL-C (mmol/l)	−0.276	2.129	0.189	0.759	0.524–1.099	0.145						
TG (mmol/l)	−0.181	0.924	0.189	0.834	0.576–1.207	0.336						
WBC (109/l)	0.056	0.880	0.060	1.057	0.941–1.188	0.348						
FIB (μg/ml)	−0.118	0.483	0.169	0.889	0.638–1.239	0.487						
DD-i (μg/ml)	0.396	0.869	0.425	1.486	0.646–3.415	0.351						
IRA												
LAD												
LCX	1.557	3.781	0.801	4.743	0.988–22.781	0.052	1.298	1.638	1.014	3.661	0.502–26.716	0.201
RCA	−0.279	0.568	0.370	0.757	0.367–1.562	0.451	−1.186	5.420	0.509	0.305	0.113–0.829	0.020
Surgery time (mins)	0.001	0.015	0.010	1.001	0.981–1.022	0.901						
Thrombus aspiration	−0.365	0.362	0.606	0.694	0.212–2.278	0.547						
Pre-dilation	−14.248	0.000	882.743	0.000	0.000-Inf	0.987						
Post-dilation	−0.044	0.013	0.386	0.957	0.449–2.039	0.908						
Stent number												
0												
1	−0.640	0.554	0.860	0.527	0.098–2.846	0.457						
2	−0.511	0.301	0.931	0.600	0.097–3.720	0.583						
Stent diameter (mm)	−0.157	0.465	0.230	0.855	0.545–1.341	0.495						
Stent length (mm)	−0.013	0.415	0.021	0.987	0.948–1.027	0.519						
Nicorandil	−0.046	0.003	0.785	0.955	0.205–4.445	0.953						
Tirofiban	0.758	1.533	0.612	2.134	0.643–7.089	0.216						

SE, standard error; OR, odds ratio; CI, confidence interval; CMD, coronary microvascular dysfunction; BMI, body mass index; HR, heart rate; SBP, systolic blood pressure; DBP. diastolic blood pressure; CAD, coronary artery disease; GDF-15, growth differentiation factor-15; NT-proBNP, N-terminal pro-brain natriuretic peptide; CK-MB, creatine kinase isoenzyme MB; hs-TnI, high-sensitivity Troponin-I; Cho, cholesterol; HDL-C, high-density lipoprotein cholesterol; LDL-C, low-density lipoprotein cholesterol; TG, triglycerides; WBC, white blood cell; FIB, fibrinogen; DD-i, D-dimer; IRA, infarct related artery; LAD, left anterior descending; LCX, left circumflex artery; RCA, right coronary artery; Inf, infinity.

5.812–104.452, $P < 0.001$) was significantly increased compared with Q1, and the trend was $P < 0.001$ (Table 3).

3.3. Expression levels of GDF-15 in different groups of patients

Firstly, we analyzed the differences in GDF-15 expression among different groups of patients, and the results showed that GDF-15 levels were significantly upregulated in the CMD group compared with the Control group (3.43 ± 1.03 ng/ml vs. 2.22 ± 1.13 ng/ml, $P < 0.001$) (Fig. 2A). GDF-15 levels were significantly higher in females than males (3.35 ± 1.25 ng/ml vs. 2.78 ± 1.19 ng/ml, $P < 0.05$) (Fig. 2B). Patients with Killip >1 had higher GDF-15 levels than those with Killip = 1 (3.48 ± 0.99 ng/ml vs. 2.83 ± 1.24 ng/ml, $P < 0.05$) (Fig. 2C), and GDF-15 levels were significantly lower in patients with LAD than LCX (3.64 ± 1.17 ng/ml vs. 2.73 ± 1.12 ng/ml, $P < 0.05$) (Fig. 2D). Although the GDF-15 levels of RCA were also lower than LCX, but there was no statistical difference (3.64 ± 1.17 ng/ml vs. 2.94 ± 1.31 ng/ml, $P = 0.06$) (Fig. 2D). In addition, no significant difference in GDF-15 levels was found in the population classified by whether they had a history of smoking, drinking, hypertension, or diabetes mellitus ($P > 0.05$) (Table S1).

3.4. Correlation analysis between the GDF-15 and other indicators

Then, we analyzed the correlation between GDF-15 and other continuity indicators, and the results showed that the GDF-15 levels were significantly positively correlated with AMR ($r = 0.50$, $P < 0.001$) (Fig. 3A) and age ($r = 0.25$, $P < 0.05$) (Fig. 3B), but were significantly negatively correlated with BMI ($r = -0.20$, $P < 0.05$) (Fig. 3C) or LDL-C ($r = -0.21$, $P < 0.05$) (Fig. 3D), but not negatively correlated with other continuity indicators (Table S2).

3.5. Subgroup analysis

To further investigate the relationship between GDF-15 and CMD in different populations, we stratified populations based on gender, age, BMI, Killip, IRA, and LDL-C levels. Multivariable logistic regression showed that there was no significant interaction between GDF-15 and CMD in different populations (all interactions were $P > 0.05$), and the GDF-15 of STEMI patients treated with PPCI was positively correlated with CMD in each subgroup, except for Killip >1 and patients with LCX IRA ($P < 0.05$), the results showed that GDF-15 was significantly positively correlated with CMD and was stable in the majority of the patients (Fig. 4).

3.6. Predictive value and incremental predictive value of GDF-15 for CMD

Univariate logistic regression of admission medical records, laboratory indexes and surgery-related data showed that gender, SBP, DBP and Killip grade were significantly correlated with CMD ($P < 0.05$), on top of that, after referring to previous studies and considering the actual needs of clinical work, the clinical baseline model (Model Without GDF-15) was constructed by including age, BMI, IRA, thrombus aspiration, LDL-C, smoking history, diabetes mellitus history and CAD family history in multivariable logistic regression extraly, and the AUC corresponding to the ROC curve was 0.788 (95 % CI: 0.712−0.864) (Fig. 5B). The ROC curve was used to evaluate the efficacy of GDF-15 in predicting CMD alone, and the results showed that its AUC was 0.782 (95 % CI: 0.704–0.861) (Fig. 5A), showing good predictive power. Then, after adding GDF-15 data on the basis of the clinical baseline model, the AUC corresponding to the ROC curve shown by the GDF-15 model (Model with GDF-15) was 0.867 (95 % CI: 0.806−0.928) (Fig. 5B), which was significantly better than that of the clinical baseline model (Δ AUC = 0.079, 95 % CI: 0.020–0.138, P = 0.009). The net reclssification improvement (NRI) results also showed that the prediction ability of the GDF-15 model was significantly improved (NRI = 0.854, 95 % CI: 0.543–1.166, P < 0.001), the integrated discrimination improvement (IDI) showed that the accuracy of the model increased by 15.1 % (IDI = 0.151, 95 % CI: 0.089–0.213, $P < 0.001$). The above results show that GDF-15 has a good prediction performance for the occurrence of CMD and has a good incremental prediction value.

Table 3
Association between the level of GDF-15 and CMD in different logistic regression models.

GDF-15 (ng/ml)	OR (95%CI)	adjusted OR (95%CI)
	Model U	Model M
GDF-15 quantile		
Q1 = 1.51 [0.11,2.05]	Reference	Reference
Q2 = 2.46 [2.07,2.97]	4.886 (1.672–14.274)*	5.830 (1.764–19.266)*
Q3 = 3.38 [2.99,4.01]	8.871 (2.91–27.042)**	7.591 (2.231–25.825)*
Q4 = 4.53 [4.01,5.04]	27.964 (7.354–106.332)**	24.639 (5.812–104.452)**
P for trend	<0.001	<0.001

GDF-15, growth differentiation factor-15; OR, odds ratio; CI, confidence interval; Model U, univariate analysis; Model M, multivariate analysis; *, $P < 0.05$; **, $P < 0.001$.

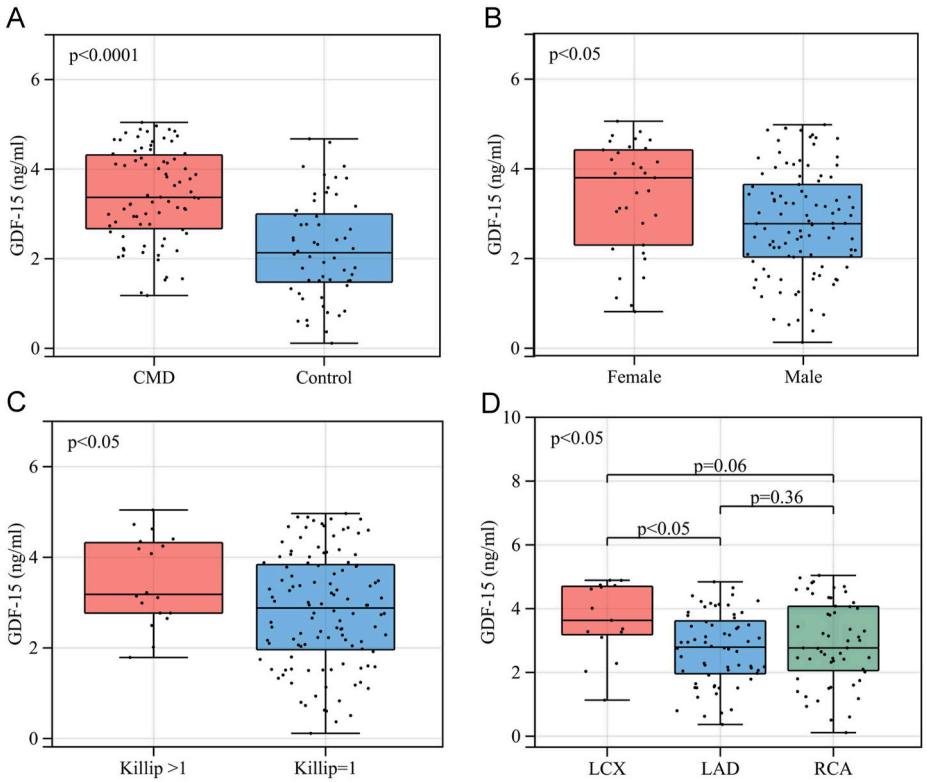

Fig. 2. GDF-15 expression level in different populations. (A) GDF-15 expression level in the CMD group was significantly higher than Control group. (B) GDF-15 expression level was significantly higher in female patients than male. (C) GDF-15 expression level in the Killip >1 group was significantly higher than the Killip = 1 group. (D) GDF-15 expression level in the LCX group was significantly higher than LAD group.

3.7. Comparison of high-level and low-level GDF-15 groups

3.7.1. Comparison of baseline data

According to the ROC curve of GDF-15 for the predicted value of CMD, the Youden index was calculated to be 0.438. The optimal cut-off value of GDF-15 for predicting CMD was 2.50 ng/ml, and the sensitivity and specificity of predicting CMD in PPCI were 0.795 and 0.643. Therefore, patients were divided into high-level group (GDF-15 $\geq$ 2.50 ng/ml) (n = 82) and low-level group (GDF-15 < 2.50 ng/ml) (n = 52) by the above optimal cut-off values of GDF-15. Baseline data comparison between the two groups was shown that the age ($P = 0.002$) and the proportion of patients with Killip >1 in the high-level group ($P = 0.010$) were significantly higher than those in the low-level group, while the levels of circulating Cho ($P = 0.029$) and LDL-C ($P = 0.023$) were significantly lower than those in the low-level group. Additionally, there were no other significant differences between the two groups (Table S3).

3.7.2. Comparison of cardiac ultrasound parameters at discharge

The results of cardiac ultrasound at discharge showed that there were no significant differences in left atrial (LA) diameter, left ventricular (LV) diameter, interventricular septum (IVS) thickness, left ventricular posterior wall (LVPW) thickness, right ventricular (RV) diameter, ascending aorta (AA) transverse diameter, pulmonary artery (PA) transverse diameter, PA pressure (PAP), E/e', LVEF and length of hospital stay (LS) between the two groups ($P > 0.05$) (Table S4).

3.7.3. Comparison of the incidence of CMD and 30-day MACE

The incidences of CMD (75.61 % vs. 30.77 %, $P < 0.001$) and 30-day MACE (26.86 % vs. 11.54 %, $P = 0.034$) in the high-level group were significantly higher than those in the low-level group (Table S5). Among them, a total of 28 patients developed MACE, including 22 cases (26.83 %) in the high-level group and 6 cases (11.54 %) in the low-level group, with a total incidence rate of 20.90 % (Table S6). The Kaplan-Meier curve was used to plot the cumulative probability of MACE in 30 days, and the results showed that the incidence of MACE in the high-level group increased significantly with the extension of observation time ($P = 0.040$) (Fig. S2).

4. Discussion

This study methodically assessed the predictive power of admission GDF-15 levels for CMD in STEMI patients undergoing PPCI. Findings revealed that higher GDF-15 levels were associated with an increased likelihood of CMD development post PPCI. GDF-15

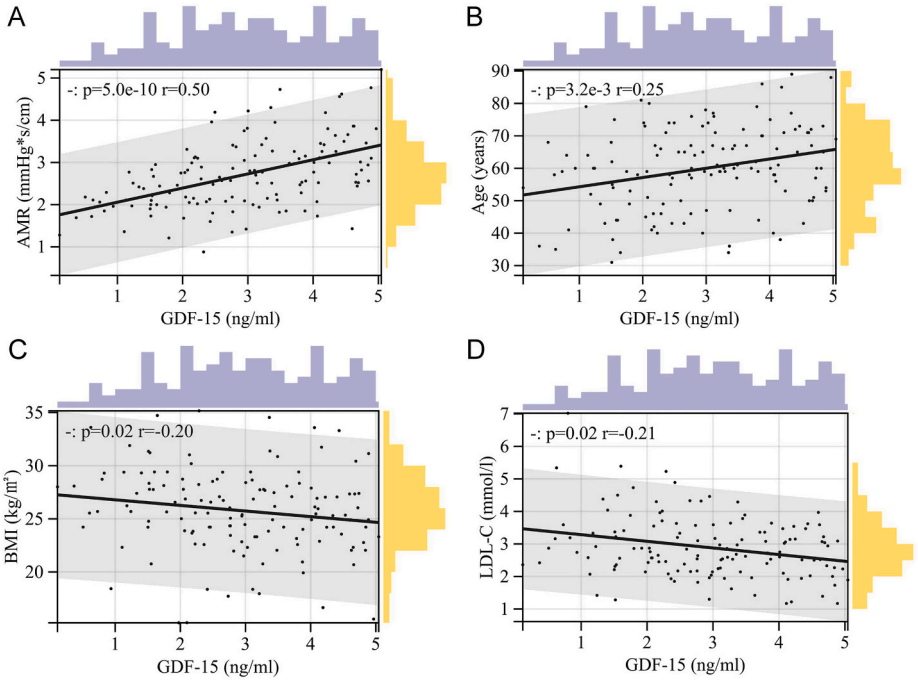

Fig. 3. Correlation analysis of GDF-15 with other indicators. (A) GDF-15 was significantly positively correlated with AMR. (B) GDF-15 was significantly positively correlated with age. (C) GDF-15 was significantly negatively correlated with BMI. (D) GDF-15 was significantly negatively correlated with LDL-C.

Subgroup analysis

Variable	Count	Percent	OR (95% CI)	P value	P for interaction
Overall	**134**	**100.0**	**2.69 (1.88 to 4.04)**	<0.001	
Gender					0.651
Male	33	24.6	3.09 (1.47 to 8.27)	0.008	
Female	101	75.4	2.49 (1.66 to 3.97)	<0.001	
Age (years)					0.571
≥60	70	52.2	2.95 (1.74 to 5.57)	<0.001	
<60	64	47.8	2.36 (1.46 to 4.17)	0.001	
BMI (kg/m²)					0.487
≥25	79	59.0	2.37 (1.55 to 3.87)	<0.001	
<25	55	41.0	3.20 (1.68 to 7.31)	0.002	
Killip					0.191
>1	18	13.4	175.40 (3.21 to 15123687.09)	0.114	
1	116	86.6	2.41 (1.68 to 3.63)	<0.001	
IRA					0.809
LAD	64	47.8	2.57 (1.52 to 4.79)	0.001	
LCX	15	11.2	1.87 (0.50 to 8.72)	0.344	
RCA	55	41.0	2.98 (1.73 to 5.92)	<0.001	
LDL-C (mmol/l)					0.360
≥2.9	59	44.0	2.26 (1.40 to 3.95)	0.002	
<2.9	75	56.0	3.24 (1.92 to 6.18)	<0.001	

Fig. 4. Subgroup analysis of the association between GDF-15 and CMD.

exhibited a significant positive association with CMD, both as a continuous and categorical variable, establishing it as an independent CMD predictor in STEMI patients following PPCI. Additionally, GDF-15 levels showed a positive correlation with patient age and an inverse relationship with BMI and LDL-C levels. Subsequent subgroup analysis and forest plots indicated that the strong positive link between GDF-15 and CMD remained consistent across various demographics, confirming GDF-15's potent correlation for CMD across diverse gender, age, BMI, and LDL-C level groups. Moreover, through the comprehensive evaluation of AUC, ΔAUC, NRI and IDI calculated by different models, it was found that GDF-15 had good predictive value and incremental value for CMD.

PPCI has emerged as the preferred method for restoring epicardial coronary flow in STEMI patients. However, a considerable

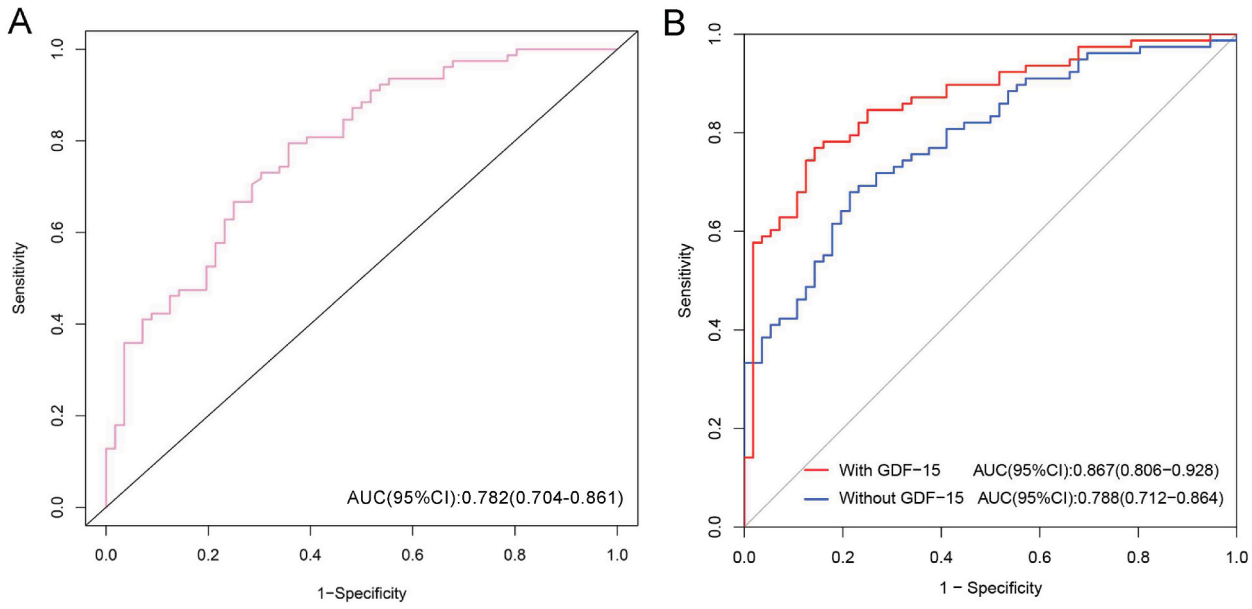

Fig. 5. The prediction efficiency of GDF-15 and different models predicted for CMD. (A) ROC curve and corresponding AUC of GDF-15. (B) ROC curves and corresponding AUCs of different models.

portion of these patients develop CMD, including the NRP, post the opening of the IRA [22]. CMD manifests as inadequate reperfusion in the distal coronary microvasculature and abnormal microvascular resistance, despite the angiographic appearance of unobstructed epicardial coronary arteries, ruling out issues like epicardial vessel dissection, spasm, or in-situ thrombosis [23]. It represents a frequent post-PPCI complication in STEMI cases. The 2017 European Society of Cardiology guidelines for STEMI management identified NRP as a critical, independent predictor of HF and mortality, highlighting the significance of the final infarct size and NRP [24]. Such enduring CMD correlates with increased in-hospital mortality following surgery, severely jeopardizing patient outcomes [25,26]. Furthermore, CMD independently forecasts left ventricular remodeling in STEMI patients undergoing PPCI, linking to negative one-year post-surgery consequences, such as HF, rehospitalization, and mortality [27,28]. Hence, early CMD detection and prevention to safeguard coronary microcirculation are imperative.

Currently, the TFG is the predominant clinical method for assessing CMD during PPCI. However, TFG's subjective nature often leads to a bias, with the left anterior descending (LAD) artery frequently rated as TIMI $\leq$2, and the right coronary artery (RCA) as TIMI 3 [29]. The cTFC offers a more objective evaluation of coronary flow during procedures, but its effectiveness is limited as the LAD's length typically surpasses that of the RCA and left circumflex artery (LCX), hindering accurate coronary microcirculation assessment [30]. Historically, invasive wire-based coronary physiological indices were the standard for CMD quantification, yet their complex nature, potential drug side effects, and high costs have restricted their clinical adoption [31]. During STEMI's acute phase, the fractional flow reserve (FFR) is prone to overestimation, potentially underrepresenting the lesion severity, making it unsuitable for IRA assessment. Advancements in coronary functional imaging have made angiography-derived coronary physiological assessments a quick, effective option for CMD evaluation [32]. The QFR has emerged as a non-invasive technique that precisely gauges myocardial ischemia severity without the need for pressure wires or drugs, thereby reducing patient risks, enhancing outcomes, and cutting healthcare costs [33,34]. QFR-guided complete revascularization shows prognostic advantages in myocardial infarction (MI) patients with multi-vessel disease [35]. Endorsements from the European Association of Percutaneous Cardiovascular Interventions and the Asia-Pacific consensus highlight its significant role in comprehensive CAD management during PCI [36–38]. At the 2020 European Association of Percutaneous Cardiovascular Intervention (EuroPCR) conference, the AMR, a new wire-free CMD assessment method based on QFR technology, was unveiled. AMR's simplicity, non-invasiveness, and cost-effectiveness make it more feasible for clinical use than CFR and IMR. When combined with artificial intelligence, AMR provides rapid, objective, and precise myocardial ischemia measurements [39]. Studies affirm AMR's strong correlation with IMR and consistent performance across varied cohorts, proving its excellent reproducibility and diagnostic accuracy [10,40,41]. Consequently, AMR was selected for CMD quantitative evaluation in this study.

In healthy individuals, serum GDF-15 levels normally range from 200 to 1200 pg/mL, with concentrations escalating with age [42]. As part of the TGF-β superfamily, GDF-15 is typically not expressed in the adult heart under normal conditions. However, myocardial damage due to heart failure, ischemia-reperfusion injury, or coronary artery atherosclerosis leads to significant GDF-15 expression by myocardial cells, adipocytes, and macrophages in the heart [43,44]. During AMI, GDF-15 levels in the bloodstream surge rapidly, establishing it as an independent risk factor for myocardial infarction [45]. Research, including studies by Khan and colleagues, indicates that elevated GDF-15 levels correlate strongly with increased Killip classification in AMI patients and serve as a prognostic marker for death and HF [46]. Distinct from other markers of myocardial injury, GDF-15 peaks within 90 min following AMI onset and

normalizes after a maximum of 52 h [47]. In light of the PPCI timing for STEMI patients, blood samples collected pre-intervention were analyzed to elucidate the relationship between GDF-15 and CMD, revealing a significant positive association. The IABP-SHOCK II trial (Intra-aortic Balloon Pump in Cardiogenic Shock II) identified admission GDF-15 levels as a crucial independent predictor of 30-day mortality for patients suffering acute myocardial infarction with cardiogenic shock (AMI-CS) [48]. Furthermore, studies by Eitel et al., employing cardiovascular magnetic resonance (CMR) imaging techniques, demonstrated that GDF-15 levels at admission robustly forecast 6-month mortality in STEMI patients receiving initial reperfusion via angioplasty [49]. Additionally, GDF-15 is one of the strongest biomarkers for predicting long-term all-cause mortality in AMI patients. When integrated with known risk factors and biomarkers, GDF-15 significantly enhances the prediction of 5-year survival rates for AMI patients [50]. Zelniker and associates have identified clinical GDF-15 thresholds (<1200 ng/L, 1200–1800 ng/L, and >1800 ng/L) that independently ascertain cardiovascular death and heart failure risks in patients with non-ST-elevation myocardial infarction (NSTEMI), facilitating early risk assessment [51]. Beyond its value in short-term and long-term prognostications, elevated GDF-15 at admission correlates with reduced blood flow during initial PPCI in STEMI patients and independently predicts the incidence of NRP following the first PPCI [52]. Our study's findings align with these observations.

Recent research has established GDF-15 as a prognostic biomarker for a range of conditions, including ischemic heart disease, heart failure, atrial fibrillation, cancer, and diabetes [53]. GDF-15 concentrations exceeding 1800 ng/L are closely linked to an increased risk of long-term major adverse cardiovascular events and all-cause mortality in CAD patients, identifying it as an independent predictor for these outcomes in the CAD population [54]. The PROVE-IT TIMI 22 trial revealed GDF-15's association with all-cause mortality, recurrent myocardial infarction, and congestive heart failure among acute coronary syndrome (ACS) patients, offering prognostic insights beyond traditional clinical predictors and other biomarkers like B-type natriuretic peptide (BNP) and high-sensitivity C-reactive protein (hs-CRP) [55]. The PLATO trial assessed GDF-15's prognostic utility in 9946 patients with non-ST-elevation acute coronary syndrome (NSTE-ACS), treated with either ticagrelor or clopidogrel, illustrating its value in benefit-risk evaluation across different treatment approaches [56]. Furthermore, GDF-15's predictive relevance in NSTE-ACS was corroborated in the GUSTO-IV and FRISC II trials, where the one-year cumulative mortality rates for patients with low, medium, and high GDF-15 levels were 1.5 %, 5.0 %, and 14.1 %, respectively. GDF-15 was predictive of cardiovascular death and myocardial infarction in non-revascularized patients, whereas it was indicative of late events in revascularized individuals [57,58]. These findings advocate for the integration of GDF-15 levels into the current cardiovascular risk assessment models, potentially enhancing risk prediction and stratification for ACS patients.

Research into the role of GDF-15 in atherosclerosis and ischemic cardiovascular diseases has progressed swiftly. In vitro experiments demonstrate that myocardial cells in the ischemic risk zone highly express GDF-15 following the ligation of mouse coronary arteries or exposure of cultured mouse cardiomyocytes to ischemia/reperfusion (I/R) injury. The associated signaling pathway is characterized by an increased production of nitric oxide (NO) synthase, triggered by ischemic hypoxia or mechanical stretch stimuli, which raises NO and peroxynitrite levels, subsequently causing an upsurge in GDF-15 expression. Conversely, during I/R, GDF-15 engages the phosphatidylinositol 3-hydroxy kinase (PI3K)/Akt pathway to diminish infarct size and mitigate myocardial damage [59,60]. Our findings corroborate that individuals with elevated GDF-15 levels are more prone to developing CMD postoperatively. Further studies suggest that the targeted delivery of growth differentiation factor-15 via extracellular vesicles enhances myocardial repair post-injury by modulating macrophage activity through the suppression of fatty acid-binding protein 4 (FABP4) expression [61]. This study also discovered that both CMD incidence and GDF-15 levels are higher in females than in males, echoing the research of Cenko and Gevaert, which may be attributable to variations in estrogen levels or endothelial function [62,63]. Our investigations additionally reveal a negative correlation between GDF-15 levels and patient BMI and LDL-C, possibly linked to GDF-15's weight-reducing properties. Overexpressed GDF-15 influences the central nervous system, curbing neuropeptide Y expression, which is associated with feeding, and enhancing anorexia-linked pro-opiomelanocortin (POMC) expression, thereby reducing appetite and body weight [64,65]. Moreover, GDF-15 plays a role in lipid metabolism and cardiovascular protection by activating the phosphoinositide 3-kinase (PI3K)/protein kinase B (PKB)/nitric oxide synthase (NOS) signaling pathway, which helps in reducing lipid accumulation, ameliorating lipid metabolism disorders, and decelerating atherosclerosis progression [66].

There are some limitations in this study: (1) As this study is a single-center study with a limited sample size, this may limit the generalizability of our findings, and a larger study is needed to validate our conclusions. (2) The participants in this study were all of yellow ethnicity, which may limit the generalizability of our findings to other races. (3) This study failed to conduct long-term follow-up of patients, so the effect of GDF-15 on the long-term prognosis of patients could not be observed. (4) The correlation between GDF-15 and postoperative CMD was only observed, but the specific mechanism is still unclear and needs to be explored in future experiments at the animal or cell level.

5. Conclusions

GDF-15 is a good biomarker for predicting the CMD in STEMI patients undergoing PPCI. And these STEMI patients with GDF-15 $\geq$ 2.50 ng/ml have a higher incidence of CMD after PPCI treatment.

Funding

This work was supported by the National Natural Science Foundation of China (82070388, 82170442 and 82370378), Taishan Scholar Program of Shandong Province (tsqn202211310 and tspd20181220), Shandong Provincial Natural Science Foundation (ZR2020MH035), National Key R&D Program of China (2020YFC1512700, 2020YFC1512705, 2020YFC1512703, 2022YFC0868600).

Data availability statement

Data will be made available on request.

CRediT authorship contribution statement

Rui Tian: Writing – original draft, Methodology. **Zerui Wang:** Formal analysis. **Shenglin Zhang:** Writing – original draft. **Xiaojun Wang:** Formal analysis. **Yiwen Zhang:** Data curation. **Jiaquan Yuan:** Data curation. **Jiajun Zhang:** Software. **Feng Xu:** Supervision, Investigation. **Yuguo Chen:** Supervision, Investigation. **Chuanbao Li:** Writing – review & editing, Project administration, Investigation, Conceptualization.

Declaration of competing interest

The authors declare that they have no known competing financial interests or personal relationships that could have appeared to influence the work reported in this paper.

Acknowledgments

Thank all the researchers who participated in this study, your contributions played a very important role in our research work. Special thanks to Mr. Zhiwei Zhang for his guidance on coronary angiography analysis. Thanks to Figdraw for providing a platform for drawing the Graphical Abstract (ID:RUUOSb91ac).

Appendix A. Supplementary data

Supplementary data to this article can be found online at https://doi.org/10.1016/j.heliyon.2024.e35476.

References

[1] T. Choudhury, N.E. West, M. El-Omar, ST elevation myocardial infarction, Clin. Med. 16 (3) (2016) 277–282, https://doi.org/10.7861/clinmedicine.16-3-277.
[2] P.G. Thrane, K.K.W. Olesen, T. Thim, et al., Mortality trends after primary percutaneous coronary intervention for ST-segment elevation myocardial infarction, J. Am. Coll. Cardiol. 82 (10) (2023) 999–1010, https://doi.org/10.1016/j.jacc.2023.06.025.
[3] J.F. Lassen, H.E. Bøtker, C.J. Terkelsen, Timely and optimal treatment of patients with STEMI, Nat. Rev. Cardiol. 10 (1) (2013) 41–48, https://doi.org/10.1038/nrcardio.2012.156.
[4] A. Durante, P.G. Camici, Novel insights into an "old" phenomenon: the no reflow, Int. J. Cardiol. 187 (2015) 273–280, https://doi.org/10.1016/j.ijcard.2015.03.359.
[5] Q. Zeng, L.D. Zhang, W. Wang, A meta-analysis of randomized controlled trials investigating tirofiban combined with conventional drugs by intracoronary administration for no-reflow prevention, Anatol. J. Cardiol. 25 (1) (2021) 7–16, https://doi.org/10.14744/AnatolJCardiol.2020.99469.
[6] C.M. Gibson, C.P. Cannon, W.L. Daley, et al., TIMI frame count: a quantitative method of assessing coronary artery flow, Circulation 93 (5) (1996) 879–888, https://doi.org/10.1161/01.cir.93.5.879.
[7] W.F. Fearon, L.B. Balsam, H.M. Farouque, et al., Novel index for invasively assessing the coronary microcirculation, Circulation 107 (25) (2003) 3129–3132, https://doi.org/10.1161/01.CIR.0000080700.98607.D1.
[8] R. Scarsini, L. Portolan, F. Della Mora, et al., Angiography-derived and sensor-wire methods to assess coronary microvascular dysfunction in patients with acute myocardial infarction, JACC Cardiovasc Imaging 16 (7) (2023) 965–981, https://doi.org/10.1016/j.jcmg.2023.01.017.
[9] C. Li, Z. Wang, H. Yang, et al., The association between angiographically derived radial wall strain and the risk of acute myocardial infarction, JACC Cardiovasc. Interv. 16 (9) (2023) 1039–1049, https://doi.org/10.1016/j.jcin.2023.02.012.
[10] Y. Fan, S. Fezzi, P. Sun, et al., In vivo validation of a novel computational approach to assess microcirculatory resistance based on a single angiographic view, J. Personalized Med. 12 (11) (2022) 1798, https://doi.org/10.3390/jpm12111798.
[11] Y. Fan, C. Li, Y. Hu, et al., Angiography-based index of microcirculatory resistance (AccuIMR) for the assessment of microvascular dysfunction in acute coronary syndrome and chronic coronary syndrome, Quant. Imag. Med. Surg. 13 (6) (2023) 3556–3568, https://doi.org/10.21037/qims-22-961.
[12] S. Desmedt, V. Desmedt, L. De Vos, J.R. Delanghe, R. Speeckaert, M.M. Speeckaert, Growth differentiation factor 15: a novel biomarker with high clinical potential, Crit. Rev. Clin. Lab Sci. 56 (5) (2019) 333–350, https://doi.org/10.1080/10408363.2019.1615034.
[13] L. Lind, L. Wallentin, T. Kempf, et al., Growth-differentiation factor-15 is an independent marker of cardiovascular dysfunction and disease in the elderly: results from the Prospective Investigation of the Vasculature in Uppsala Seniors (PIVUS) Study, Eur. Heart J. 30 (19) (2009) 2346–2353, https://doi.org/10.1093/eurheartj/ehp261.
[14] F. Rueda, J. Lupón, C. García-García, et al., Acute-phase dynamics and prognostic value of growth differentiation factor-15 in ST-elevation myocardial infarction, Clin. Chem. Lab. Med. 57 (7) (2019) 1093–1101, https://doi.org/10.1515/cclm-2018-1189.
[15] A. Garcia-Osuna, J. Sans-Rosello, A. Ferrero-Gregori, A. Alquezar-Arbe, A. Sionis, J. Ordóñez-Llanos, Risk assessment after ST-segment elevation myocardial infarction: can biomarkers improve the performance of clinical variables? J. Clin. Med. 11 (5) (2022) 1266, https://doi.org/10.3390/jcm11051266.
[16] B. Gandevia, A. Tovell, Declaration of helsinki, Med. J. Aust. 2 (1964) 320–321.
[17] K. Thygesen, J.S. Alpert, A.S. Jaffe, et al., Fourth universal definition of myocardial infarction (2018), Glob Heart 13 (4) (2018) 305–338, https://doi.org/10.1016/j.gheart.2018.08.004.
[18] A.M. Maznyczka, K.G. Oldroyd, P. McCartney, M. McEntegart, C. Berry, The potential use of the index of microcirculatory resistance to guide stratification of patients for adjunctive therapy in acute myocardial infarction, JACC Cardiovasc. Interv. 12 (10) (2019) 951–966, https://doi.org/10.1016/j.jcin.2019.01.246.
[19] S. Tu, M. Echavarria-Pinto, C. von Birgelen, et al., Fractional flow reserve and coronary bifurcation anatomy: a novel quantitative model to assess and report the stenosis severity of bifurcation lesions, JACC Cardiovasc. Interv. 8 (4) (2015) 564–574, https://doi.org/10.1016/j.jcin.2014.12.232.
[20] S. Tu, J. Westra, J. Yang, et al., Diagnostic accuracy of fast computational approaches to derive fractional flow reserve from diagnostic coronary angiography: the international multicenter FAVOR pilot study, JACC Cardiovasc. Interv. 9 (19) (2016) 2024–2035, https://doi.org/10.1016/j.jcin.2016.07.013.

[21] Chinese Society of Cardiology of Chinese Medical Association, Editorial board of Chinese journal of Cardiology, Zhonghua Xinxueguanbing Zazhi 47 (10) (2019) 766–783, https://doi.org/10.3760/cma.j.issn.0253-3758.2019.10.003.
[22] A. Koller, M.H. Laughlin, E. Cenko, et al., Functional and structural adaptations of the coronary macro- and microvasculature to regular aerobic exercise by activation of physiological, cellular, and molecular mechanisms: ESC Working Group on Coronary Pathophysiology and Microcirculation position paper, Cardiovasc. Res. 118 (2) (2022) 357–371, https://doi.org/10.1093/cvr/cvab246.
[23] G. Niccoli, G. Scalone, A. Lerman, F. Crea, Coronary microvascular obstruction in acute myocardial infarction, Eur. Heart J. 37 (13) (2016) 1024–1033, https://doi.org/10.1093/eurheartj/ehv484.
[24] T.F. Lüscher, ST-segment elevation myocardial infarction: the new ESC Guidelines, Eur. Heart J. 39 (2) (2018) 75–78, https://doi.org/10.1093/eurheartj/ehx792.
[25] G. Niccoli, R.A. Montone, B. Ibanez, et al., Optimized treatment of ST-elevation myocardial infarction, Circ. Res. 125 (2) (2019) 245–258, https://doi.org/10.1161/CIRCRESAHA.119.315344.
[26] R.A. Montone, V. Vetrugno, G. Santacroce, et al., Recurrence of angina after ST-segment elevation myocardial infarction: the role of coronary microvascular obstruction, Eur Heart J Acute Cardiovasc Care (2019) 2048872619880661, https://doi.org/10.1177/2048872619880661.
[27] T. Padro, O. Manfrini, R. Bugiardini, et al., ESC Working Group on Coronary Pathophysiology and Microcirculation position paper on 'coronary microvascular dysfunction in cardiovascular disease', Cardiovasc. Res. 116 (4) (2020) 741–755, https://doi.org/10.1093/cvr/cvaa003.
[28] A. Kali, I. Cokic, R. Tang, et al., Persistent microvascular obstruction after myocardial infarction culminates in the confluence of ferric iron oxide crystals, proinflammatory burden, and adverse remodeling, Circ Cardiovasc Imaging 9 (11) (2016) e004996, https://doi.org/10.1161/CIRCIMAGING.115.004996.
[29] M.J. Butler, W. Chan, A.J. Taylor, A.M. Dart, S.J. Duffy, Management of the no-reflow phenomenon, Pharmacol. Ther. 132 (1) (2011) 72–85, https://doi.org/10.1016/j.pharmthera.2011.05.010.
[30] C.M. Gibson, C.P. Cannon, W.L. Daley, et al., TIMI frame count: a quantitative method of assessing coronary artery flow, Circulation 93 (5) (1996) 879–888, https://doi.org/10.1161/01.cir.93.5.879.
[31] C.C.Y. Wong, T. Nishi, A.S.C. Yong, et al., Discordance between the index of microcirculatory resistance and coronary flow reserve after percutaneous coronary intervention, JACC Cardiovasc. Interv. 14 (21) (2021) 2412–2414, https://doi.org/10.1016/j.jcin.2021.07.053.
[32] J. Wu, A.D. Lu, L.P. Zhang, Y.X. Zuo, Y.P. Jia, Zhonghua Xue Ye Xue Za Zhi 40 (1) (2019) 52–57, https://doi.org/10.3760/cma.j.issn.0253-2727.2019.01.010.
[33] B. Xu, S. Tu, L. Song, et al., Angiographic quantitative flow ratio-guided coronary intervention (FAVOR III China): a multicentre, randomised, sham-controlled trial, Lancet 398 (10317) (2021) 2149–2159, https://doi.org/10.1016/S0140-6736(21)02248-0.
[34] D. Ang, C. Berry, FAVOR III China: quantitative flow ratio-guided coronary intervention in practice, Cardiovasc. Res. 118 (11) (2022) e78–e80, https://doi.org/10.1093/cvr/cvac109.
[35] S. Biscaglia, V. Guiducci, J. Escaned, et al., Complete or culprit-only PCI in older patients with myocardial infarction, N. Engl. J. Med. 389 (10) (2023) 889–898, https://doi.org/10.1056/NEJMoa2300468.
[36] J. Escaned, C. Berry, Bruyne B. De, et al., Applied coronary physiology for planning and guidance of percutaneous coronary interventions. A clinical consensus statement from the European Association of Percutaneous Cardiovascular Interventions (EAPCI) of the European Society of Cardiology, EuroIntervention 19 (6) (2023) 464–481, https://doi.org/10.4244/EIJ-D-23-00194.
[37] B.K. Koo, J.M. Lee, D. Hwang, et al., Practical application of coronary physiologic assessment: asia-pacific expert consensus document: Part 1, JACC Asia 3 (5) (2023) 689–706, https://doi.org/10.1016/j.jacasi.2023.07.003.
[38] B.K. Koo, D. Hwang, S. Park, et al., Practical application of coronary physiologic assessment: asia-pacific expert consensus document: Part 2, JACC Asia 3 (6) (2023) 825–842, https://doi.org/10.1016/j.jacasi.2023.07.004.
[39] Y. Fan, S. Fezzi, P. Sun, et al., In vivo validation of a novel computational approach to assess microcirculatory resistance based on a single angiographic view, J. Personalized Med. 12 (11) (2022) 1798, https://doi.org/10.3390/jpm12111798.
[40] E. Fernández-Peregrina, H.M. Garcia-Garcia, J. Sans-Rosello, et al., Angiography-derived versus invasively-determined index of microcirculatory resistance in the assessment of coronary microcirculation: a systematic review and meta-analysis, Cathet. Cardiovasc. Interv. 99 (7) (2022) 2018–2025, https://doi.org/10.1002/ccd.30174.
[41] B. Gao, G. Wu, J. Xie, et al., Quantitative flow ratio-derived index of microcirculatory resistance as a novel tool to identify microcirculatory function in patients with ischemia and No obstructive coronary artery disease, Cardiology 149 (1) (2024) 14–22, https://doi.org/10.1159/000534287.
[42] T. Kempf, R. Horn-Wichmann, G. Brabant, et al., Circulating concentrations of growth-differentiation factor 15 in apparently healthy elderly individuals and patients with chronic heart failure as assessed by a new immunoradiometric sandwich assay, Clin. Chem. 53 (2) (2007) 284–291, https://doi.org/10.1373/clinchem.2006.076828.
[43] J. Xu, T.R. Kimball, J.N. Lorenz, et al., GDF15/MIC-1 functions as a protective and antihypertrophic factor released from the myocardium in association with SMAD protein activation, Circ. Res. 98 (3) (2006) 342–350, https://doi.org/10.1161/01.RES.0000202804.84885.d0.
[44] T. Kempf, E. Björklund, S. Olofsson, et al., Growth-differentiation factor-15 improves risk stratification in ST-segment elevation myocardial infarction, Eur. Heart J. 28 (23) (2007) 2858–2865, https://doi.org/10.1093/eurheartj/ehm465.
[45] N. Schaub, T. Reichlin, R. Twerenbold, et al., Growth differentiation factor-15 in the early diagnosis and risk stratification of patients with acute chest pain, Clin. Chem. 58 (2) (2012) 441–449, https://doi.org/10.1373/clinchem.2011.173310.
[46] S.Q. Khan, K. Ng, O. Dhillon, et al., Growth differentiation factor-15 as a prognostic marker in patients with acute myocardial infarction, Eur. Heart J. 30 (9) (2009) 1057–1065, https://doi.org/10.1093/eurheartj/ehn600.
[47] T. Stiermaier, V. Adams, M. Just, et al., Growth differentiation factor-15 in Takotsubo cardiomyopathy: diagnostic and prognostic value, Int. J. Cardiol. 173 (3) (2014) 424–429, https://doi.org/10.1016/j.ijcard.2014.03.014.
[48] G. Fuernau, C. Poenisch, I. Eitel, et al., Growth-differentiation factor 15 and osteoprotegerin in acute myocardial infarction complicated by cardiogenic shock: a biomarker substudy of the IABP-SHOCK II-trial, Eur. J. Heart Fail. 16 (8) (2014) 880–887, https://doi.org/10.1002/ejhf.117.
[49] I. Eitel, P. Blase, V. Adams, et al., Growth-differentiation factor 15 as predictor of mortality in acute reperfused ST-elevation myocardial infarction: insights from cardiovascular magnetic resonance, Heart 97 (8) (2011) 632–640, https://doi.org/10.1136/hrt.2010.219543.
[50] E. Skau, E. Henriksen, P. Wagner, P. Hedberg, A. Siegbahn, J. Leppert, GDF-15 and TRAIL-R2 are powerful predictors of long-term mortality in patients with acute myocardial infarction, Eur J Prev Cardiol 24 (15) (2017) 1576–1583, https://doi.org/10.1177/2047487317725017.
[51] T.A. Zelniker, P. Jarolim, M.G. Silverman, et al., Prognostic role of GDF-15 across the spectrum of clinical risk in patients with NSTE-ACS, Clin. Chem. Lab. Med. 57 (7) (2019) 1084–1092, https://doi.org/10.1515/cclm-2018-1081.
[52] O. Dogdu, Assessment of growth differentiation factor 15 levels on coronary flow in patients with STEMI undergoing primary PCI, Diseases 8 (2) (2020) 16, https://doi.org/10.3390/diseases8020016.
[53] E.T. Kato, D.A. Morrow, J. Guo, et al., Growth differentiation factor 15 and cardiovascular risk: individual patient meta-analysis, Eur. Heart J. 44 (4) (2023) 293–300, https://doi.org/10.1093/eurheartj/ehac577.
[54] M. Li, L. Duan, Y.L. Cai, et al., Growth differentiation factor-15 is associated with cardiovascular outcomes in patients with coronary artery disease, Cardiovasc. Diabetol. 19 (1) (2020) 120, https://doi.org/10.1186/s12933-020-01092-7.
[55] M.P. Bonaca, D.A. Morrow, E. Braunwald, et al., Growth differentiation factor-15 and risk of recurrent events in patients stabilized after acute coronary syndrome: observations from PROVE IT-TIMI 22, Arterioscler. Thromb. Vasc. Biol. 31 (1) (2011) 203–210, https://doi.org/10.1161/ATVBAHA.110.213512.
[56] L. Wallentin, D. Lindholm, A. Siegbahn, et al., Biomarkers in relation to the effects of ticagrelor in comparison with clopidogrel in non-ST-elevation acute coronary syndrome patients managed with or without in-hospital revascularization: a substudy from the Prospective Randomized Platelet Inhibition and Patient Outcomes (PLATO) trial, Circulation 129 (3) (2014) 293–303, https://doi.org/10.1161/CIRCULATIONAHA.113.004420.
[57] K.C. Wollert, T. Kempf, B. Lagerqvist, et al., Growth differentiation factor 15 for risk stratification and selection of an invasive treatment strategy in non ST-elevation acute coronary syndrome, Circulation 116 (14) (2007) 1540–1548, https://doi.org/10.1161/CIRCULATIONAHA.107.697714.

[58] K.C. Wollert, T. Kempf, T. Peter, et al., Prognostic value of growth-differentiation factor-15 in patients with non-ST-elevation acute coronary syndrome, Circulation 115 (8) (2007) 962–971, https://doi.org/10.1161/CIRCULATIONAHA.106.650846.
[59] T. Kempf, M. Eden, J. Strelau, et al., The transforming growth factor-beta superfamily member growth-differentiation factor-15 protects the heart from ischemia/reperfusion injury, Circ. Res. 98 (3) (2006) 351–360, https://doi.org/10.1161/01.RES.0000202805.73038.48.
[60] T. Kempf, A. Zarbock, C. Widera, et al., GDF-15 is an inhibitor of leukocyte integrin activation required for survival after myocardial infarction in mice, Nat. Med. 17 (5) (2011) 581–588, https://doi.org/10.1038/nm.2354.
[61] Xiao T, Wei J, Cai D, et al. Extracellular vesicle mediated targeting delivery of growth differentiation factor-15 improves myocardial repair by reprogramming macrophages post myocardial injury. Biomed. Pharmacother. doi:10.1016/j.biopha.2024.116224.
[62] E. Cenko, B. Ricci, S. Kedev, et al., The no-reflow phenomenon in the young and in the elderly, Int. J. Cardiol. 222 (2016) 1122–1128, https://doi.org/10.1016/j.ijcard.2016.07.209.
[63] S.A. Gevaert, D. De Bacquer, P. Evrard, et al., Gender, TIMI risk score and in-hospital mortality in STEMI patients undergoing primary PCI: results from the Belgian STEMI registry, EuroIntervention 9 (9) (2014) 1095–1101, https://doi.org/10.4244/EIJV9I9A184.
[64] N.J. Michael, S.E. Simonds, M. van den Top, M.A. Cowley, D. Spanswick, Mitochondrial uncoupling in the melanocortin system differentially regulates NPY and POMC neurons to promote weight-loss, Mol. Metabol. 6 (10) (2017) 1103–1112, https://doi.org/10.1016/j.molmet.2017.07.002.
[65] V.W. Tsai, R. Manandhar, S.B. Jørgensen, et al., The anorectic actions of the TGFβ cytokine MIC-1/GDF15 require an intact brainstem area postrema and nucleus of the solitary tract, PLoS One 9 (6) (2014) e100370, https://doi.org/10.1371/journal.pone.0100370.
[66] J. Li, L. Yang, W. Qin, G. Zhang, J. Yuan, F. Wang, Adaptive induction of growth differentiation factor 15 attenuates endothelial cell apoptosis in response to high glucose stimulus, PLoS One 8 (6) (2013) e65549, https://doi.org/10.1371/journal.pone.0065549.